A NEW MODEL FOR CAVITATION INDUCED PRIMARY BREAK-UP OF DIESEL SPRAYS

C. Baumgarten, J. Stegemann and G. P. Merker
baumgarten@itv.uni-hannover.de
Institut für Technische Verbrennung, Universität Hannover,
Welfengarten 1A, 30167 Hannover, Germany

Abstract
In the case of high pressure diesel injection the flow conditions inside the injection holes have an important influence on the development of the spray. The existence of cavitation structures is known to contribute to the instantaneous break-up of the liquid when it leaves the nozzle. Today the majority of CFD-codes use an Eulerian /Lagrangeian way of description in order to calculate the temporal and spatial distribution of the continuous gas phase and the dispersed liquid. Because of the Lagrangeian way to track the liquid the spray calculation starts with big spherical fuel droplets that are subject to secondary aerodynamic induced break-up. The origin of these drops (primary break-up) is usually not modelled but replaced by assumptions. Today it is well known that this method of treating the primary break-up is not sufficient at all and that the primary break-up in the near nozzle region is mainly dependent on the flow conditions inside the injection holes. In this paper a new model for cavitation and turbulence induced primary break-up is presented, which is able to map the influence of the cavitating nozzle flow on spray break-up. Different locations and sizes of both vapour and liquid zones inside the injection holes lead to different spray structures and cone angles near the nozzle. The model includes cavitation bubble dynamics. It describes the transition from the cavitating flow inside the injection hole to the dense spray near the nozzle and provides all necessary starting conditions for the spray simulation like spray cone angle, drop sizes, velocities etc. The Kelvin-Helmholtz model is used to calculate the secondary break-up. The model has been implemented in the 3-d-CFD code KIVA-3V and a first validation has been done.

Introduction

In direct injection diesel engines the fuel atomization process strongly affects combustion and exhaust emissions [1]. Fig.1 shows details of the disintegration process which is divided into the primary and the secondary break-up. The primary break-up is the first disintegration of the coherent liquid into big droplets and ligaments near the nozzle. It strongly depends on the flow conditions inside the injection holes that give the starting conditions for the spray break-up. In the case of high pressure injection the presence of cavitation makes the disintegration already begin inside the holes: because of the strong acceleration of the fuel at the inlet of the holes the static pressure decreases considerably. The curvature of the streamlines superimposes an additional radial pressure gradient because of centrifugal forces [2]. At the inlet edge the pressure falls to the vapour pressure resulting in the formation of cavitation structures along the walls. These cavitation structures extend to the exit, leave the nozzle and collapse outside (Fig.1). This results in instantaneous break-up and spray divergence. The turbulent and cavitating nozzle flow has been recognized as the most important influence parameter on the primary break-up in the case of high pressure diesel injection [2,3,4]. The secondary break-up is the further break-up of droplets into smaller ones. Because of the relative velocity between droplet and gas aerodynamic forces make surface waves grow which are then split off and generate small droplets.

Today quite sophisticated models for the description of the secondary break-up like Taylor Analogy, Kelvin-Helmholtz and Rayleigh-Taylor Break-up are implemented in modern CFD-codes. The Lagrangeian way to describe the liquid implies the existence of drops. In order to describe the transition from the coherent liquid inside the nozzle to the primary droplets, sub-models have to be used. Usually uniform droplets whose diameter is equal to the nozzle diameter are assumed to leave the nozzle (Fig.1, blob-method). The starting conditions of these blobs have to be adjusted for each calculation in order to get reasonable results. The influence of the cavitating nozzle flow on the drop size distribution, the spray angle etc. cannot be mapped satisfying.

Arcoumanis et al. [5] have developed a cavitation induced atomization model which uses the total area at the exit of the injection hole occupied by cavitation bubbles to calculate the radius of an equivalent bubble having the same area as all bubbles together. The collapse time of this artificial bubble is used as time scale for the atomization process. The collapse energy which contributes to the production of droplets in the primary break-up zone is not included.

Huh and Gosman [6] have published a phenomenological model based on the assumption that cavitation and turbulence inside the nozzle holes can be attributed to turbulent fluctuations in the exit flow being the dominant

source of perturbations to the free surface. The analysis reproduces measured spray angles tolerably well. However the effects of cavitation are represented in a very crude fashion.

Nishimura and Assanis [7] have presented a model for primary atomization based on cavitation bubble collapse energy. It tracks bubble dynamics inside the injector and transfers collapse energy to turbulent kinetic energy. The latter induces an additional break-up force that is balanced with aerodynamic and surface tension forces to determine primary break-up time and total mass of child droplets. The model gives good results but is not able to map the influence of flow asymmetries inside the holes on the 3-d primary spray.

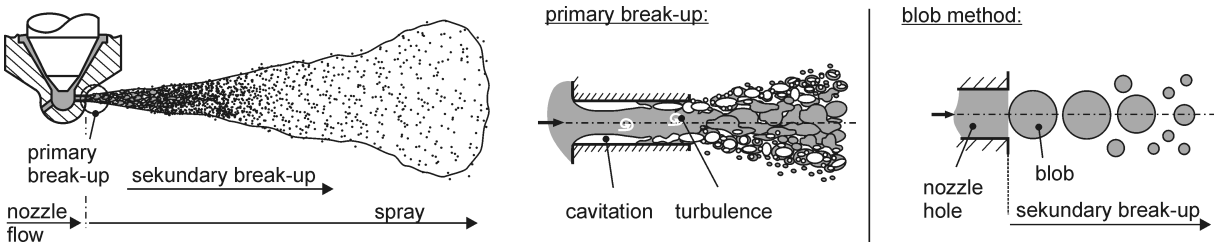

Figure 1: Cavitation induced primary break-up (high pressure diesel injection) and blob-method

In order to develop an improved primary break-up model for high pressure diesel injection detailed experimental and numerical investigations of the nozzle hole flow have been performed [8]. These investigations have shown that during the quasi-stationary injection phase (full needle lift) there is a stationary distribution of cavitation and liquid regions. Thus the flow can be divided into two zones (Fig. 2): zone 1 (liquid, high momentum) and zone 2 (mixture of cavitation bubbles and liquid ligaments, low momentum). The shape, extension and position of the zones is strongly dependent on the nozzle geometry. Fig. 2 shows the two-zone distribution for an axis-symmetric (geometry A) and a non-axis-symmetric single hole nozzle (geometry B). Details about the exact geometries are published in [8]. In case of geometry A the exit flow consists of an inner liquid flow surrounded by the cavitation zone. This leads to a symmetric primary spray. In case of geometry B the cavitation zone is concentrated at the upper wall resulting in a larger divergence of the upper part of the primary spray. Both geometries are used in this paper to study the behaviour of the new primary break-up model.

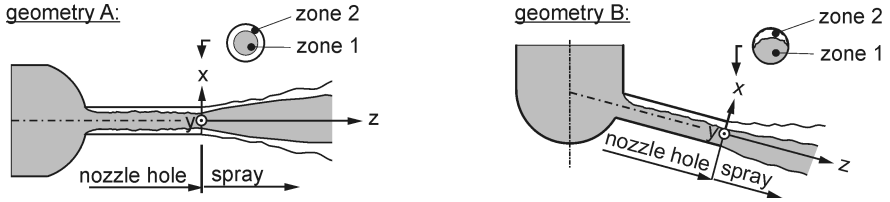

Figure 2: Two-zone structure of nozzle hole flow

Primary break-up model

The purpose of the new primary break-up model is to describe the transition from the flow inside the nozzle to the first primary droplets and to provide all starting conditions for the calculation of secondary break-up and spray formation. The input data for the new model like average flow velocity u of the liquid zone, extension, shape and position of liquid (zone 1) and cavitation (zone 2), mass flow of both zones and the average void fraction $\alpha = (\rho - \rho_l)/(\rho_v - \rho_l)$ of zone 2 are extracted from a CFD calculation of the nozzle hole flow. The indices "v" and "l" indicate vapour and liquid, ρ is the average density.

Fig. 3 shows the structure of the primary break-up model. The model assumes that the primary break-up begins already inside the nozzle and that large cylindrical primary ligaments of length L and Diameter D leave the nozzle hole. D is equal to the nozzle diameter and L is equal to the effective diameter of the liquid zone ($d_{eff} = (4\ area_{zone1}/\pi)^{0,5}$). Smaller areas of zone 1 result in shorter primary ligaments and represent an increased part of the primary break-up that has already taken place inside the nozzle.

According to the two-zone nozzle hole flow the primary ligaments also consist of two zones whose distribution is equal to the one at the nozzle exit. The flow velocity u in axial direction is the average velocity of the liquid zone at the nozzle exit. Because the stochastic parcel method is used to simulate the spray break-up process, all cavitation bubbles inside a primary ligament have the same size, but from ligament to ligament the sizes differ. No detailed experimental data about bubble sizes is available in the literature, and a size distribution has to be assumed. For the investigations described in this paper bubble sizes are sampled from a Gaussian distribution ($\bar{r}$ = 10 µm, std.dev.:10 µm), but only the part of the curve between a minimum radius of 2 µm and a maximum one of $L_{cav,\ max}/2$ is used ($L_{cav,\ max}$: see Fig. 4). From the known average void fraction and size of zone

2 the volume of pure vapour and the number of bubbles inside a primary ligament can be calculated. The calculation of bubble dynamics gives the total collapse energy E_{cav} and the bubble collapse time t_{coll} .

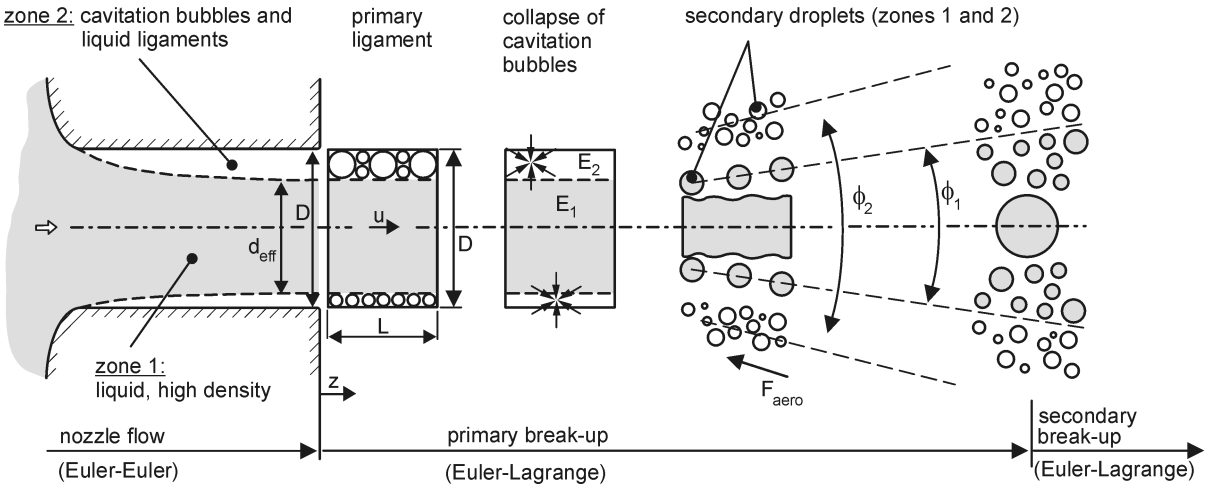

Figure 3: Structure of the new two-zone primary break-up model

The break-up of the primary ligament into secondary droplets is assumed to occur at the time t_{coll} after leaving the nozzle. Furthermore it is assumed that the bubble collapse is homogeneously distributed in zone 2 and that it results in pressure waves which propagate to the interfaces. At the interface between gas and zone 2 the collapse energy E_{cav2} reinforces the break-up of zone 2. At the interface between zone 2 and zone 1 the energy E_{cav1} is absorbed from zone 1 and contributes to the break-up of the liquid. The ratio E_{cav2}/E_{cav1} is therefore calculated as area of the interface between gas and zone 2 divided by the one between zone 1 and zone 2. The larger the cavitation zone, the bigger the part of energy that is available for the break-up of zone 2. A concentration of a fixed volume of zone 2 e.g. at the upper wall (Fig. 2, geometry B) also makes the ratio E_{cav2}/E_{cav1} increase compared with the symmetric case (geometry A). The averaged turbulent kinetic energies (E_{turb1} and E_{turb2}) of each zone, that are created inside the nozzle hole, also contribute to the primary break-up outside the nozzle. The final energies available for break-up of zone 1 and zone 2 (E_1 and E_2, see Fig. 3) are calculated as

$$E_1 = E_{cav1} + E_{turb1} \quad (1a), \quad E_2 = E_{cav2} + E_{turb2} \quad (1b) \quad . \tag{1}$$

Break-up of zone 2:

The break-up energy E_2 is used to produce small droplets (surface energy E_{surf2}) with a velocity component perpendicular to the spray axis (kinetic energy E_{kin2}, spray angle ϕ_2, see Fig. 3). An empirical constant

$$\kappa = E_{surf\,2} / E_{kin\,2} \quad (2a), \quad E_{surf\,2} + E_{kin\,2} = E_2 \quad (2b) \tag{2}$$

is used in order to estimate the part of energy E_{surf2} available for the production of new secondary droplets (secondary droplets: index "sec2", σ: surface tension) as well as the part of energy E_{kin2} available for spray angle

$$E_{surf\,2} = \sigma\pi d_{sec\,2}^2 n_2 \quad (3a) \quad \text{with} \quad n_2 = mass_{zone2} / mass_{drop,sec\,2} \quad (3b) \tag{3}$$

$$E_{kin\,2} = 0{,}5 mass_{drop,sec\,2} v_{radial}^2 n_2 \quad (4a), \quad \phi_2 = 2\,atan(v_{radial} / v_{axial}) \quad (4b) \,. \tag{4}$$

Combining eq. (3a) and (3b) d_{sec} and n_2 can be calculated. The axial velocity v_{axial} of the new droplets is identical with the one of the primary ligament before break-up. The axial velocity of primary ligaments and secondary droplets is only reduced by momentum transfer to the gas between break-up (F_{aero}, Fig. 3). Finally, the direction of the secondary droplets in the x-y plane perpendicular to the spray axis must be calculated. It is obvious that the circumferential distribution $L_{cav}(\varphi)$ of zone 2 (Fig. 4) directly influences the distribution of collapse energy and thus the production of droplets. The probability $P(\varphi)$ of new secondary droplets to be created at a certain position φ is assumed to be proportional to the thickness $L_{cav}(\varphi)$ of zone 2. The droplets are assumed to move radial outwards with velocity v_{radial}. Because the stochastic parcel method is used, zone 2 will break up in only one secondary parcel containing small droplets with identical size. The circumferential position φ of the parcel is sampled from the probability density function $P(\varphi)$. This method to model the primary spray angle ϕ_2 of zone 2 results in larger spray divergence at circumferential positions φ where there is a concentration of collapse energy and in small or even no divergence at positions with small or zero thickness of zone 2. All in all a 3-d spray distribution of zone 2 is obtained. The small secondary droplets will form the outer zone of the

primary spray region. This zone does not contain much mass but will lead to an optical dense and strongly diverging primary spray. The small droplets of zone 2 are subject to aerodynamic forces. They will decelerate fast and undergo further Kelvin-Helmholtz break-up.

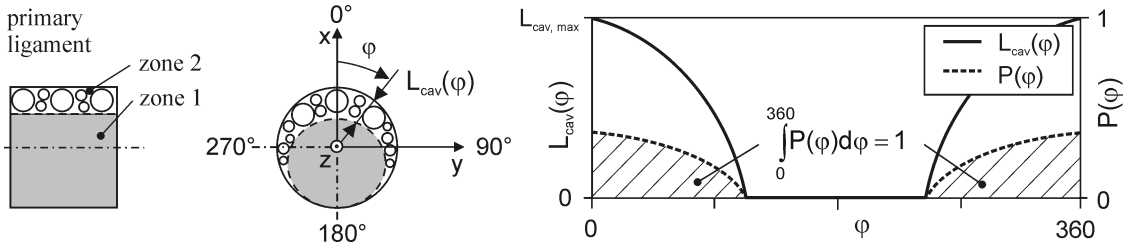

Figure 4: The probability P(φ) for a secondary parcel of zone 2 to be emitted at a position φ is dependent on the circumferential distribution $L_{cav}(\varphi)$ of the cavitation zone itself

Break-up of zone 1:

Zone 1 consists of pure liquid with high momentum in axial direction. Assuming isotropic turbulence, the energy E_1 available for break-up results in a turbulent velocity

$$u_{turb1} = (2E_1 / 3\,mass_{zone1})^{0,5} \tag{5}$$

inside zone 1. Zone 1 will break up immediately after the disintegration of zone 2. Similar to the modelling in [10] it is assumed that the turbulent velocity fluctuations induce a deformation force on the surface of zone 1

$$F_{turb1} = \text{dynamic pressure} \cdot \text{surface area} = \pi d_{zone1} L(\rho_1 / 2) u_{turb1}^2 . \tag{6}$$

Mass is split off until the surface tension force

$$F_{surf\,1} = 2\sigma(d_{zone1} + L) \tag{7}$$

is equal to F_{turb1}. The new diameter of the remaining cylindrical parent ligament is then calculated as

$$d_{parent1} = 2\sigma L /(\pi L \rho_1 E_1 /(3\,mass_{zone1}) - 2\sigma) \quad . \tag{8}$$

After break-up the cylindrical parent drop is transferred to a spherical drop. From the remaining turbulent energy inside the drop the one to form its surface is subtracted. The rest is transferred into kinetic energy perpendicular to the spray axis. But not all of the latter energy is available. Because the spray of zone 1 is very dense (it contains most of the total spray mass) the probability of droplet interactions with dissipation and loss of energy is much higher than in zone 2. In contrast to the break-up calculation of zone 2, where the efficiency η_2 of the energy transformation is assumed to be 1 and thus is not mentioned above, an efficiency $\eta_{parent1}$ is now sampled from a uniform distribution between 0 and 1 and the energy available for spray divergence is reduced. The direction φ of the parent parcel in the x-y-plane is sampled from a uniform distribution between 0° and 360°.

The turbulent kinetic energy of the split mass of zone 1 (child parcel) is the maximum energy available for new surface and spray angle ϕ_1. Because the break-up occurs in the very dense zone, again an efficiency η_{child1} is sampled from a uniform distribution between 0 and 1 and the break-up energy is reduced. Then the same energy ratio κ as in zone 2 is used to estimate the amount of surface and kinetic energy and to calculate the droplet size and radial velocity (eq. (2)-(4)). In the case of η = 1 small droplets with maximum spray angle ϕ_1 will be produced. In the case of η = 0 the split mass will form one big droplet with no radial velocity component. The direction φ of the child parcel in the x-y-plane is again sampled from a uniform distribution between 0° and 360°. All in all this method to calculate the break-up of zone 1 results in a symmetric solid cone spray with high axial momentum and big droplets. Zone 1 will have a higher penetration and govern the spray properties in the far field of the nozzle. All secondary droplets of zone 1 are subject to Kelvin-Helmholtz break-up.

Cavitation bubble dynamics:

It is assumed that the bubbles leaving the nozzle experience a sudden pressure rise from the vapour pressure p_v to the pressure p_∞ of the gas inside the combustion chamber and collapse inside zone 2. The equation of Herring and Trilling [9] is used to calculate the bubble dynamics during collapse:

$$(1 - \frac{2\dot{R}}{a})R\ddot{R} + \frac{3}{2}(1 - \frac{4\dot{R}}{3a})\dot{R}^2 = \frac{1}{\rho_\infty}(p_v - \frac{2\sigma}{R} - \frac{4\eta}{R}\dot{R} - p_\infty) \quad . \tag{9}$$

R is the bubble radius, $\dot{R}$ and $\ddot{R}$ are the time dependent velocity and acceleration of the bubble wall. The modelling accounts for the effect of a compressible environment (acoustic approximation, a: average sound

speed of zone 2) on the collapse process. Furthermore the effect of surface tension σ and liquid viscosity η are included and p_v is the vapour pressure of diesel fuel. p_∞ and ρ_∞ are the static pressure and the density of the environment (zone 2). The kinetic energy of the fluid surrounding the bubble can be estimated as [10]

$$E = 2\pi\rho_\infty \dot{R}^2 R^3 \quad . \tag{10}$$

Using a value of a = ∞, eq. (9) reduces to the better known equation of Rayleigh, Plesset, Noltingk, Neppiras and Poritsky (RPNNP-equation) which describes the bubble dynamics in an incompressible environment.

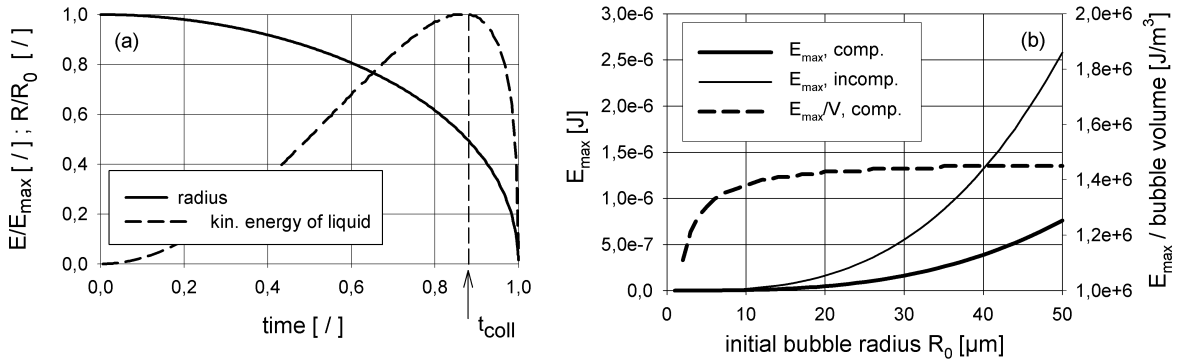

a	[m/s]	90	sound speed, zone 2
ρ_∞	[kg/m^3]	360	density, zone 2
η	[kg/m s]	$2{,}52 \cdot 10^{-3}$	dynamic viscosity of fuel
σ	[N/m]	$21{,}1 \cdot 10^{-3}$	surface tension
p_v	[Pa]	2100	vapour pressure of fuel
p_∞	[MPa]	5	back pressure

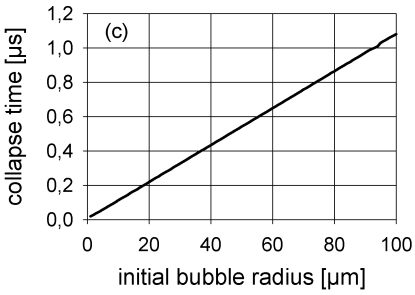

Table 1: Boundary conditions for the calculation of bubble dynamics

Figure 5: (a) Representative curves of bubble radius and kinetic energy during collapse, (b) Maximum collapse energy as function of initial bubble radius, (c) Collapse time as function of initial bubble radius

In Fig. 5(a) the non-dimensionalized curves of radius and kinetic energy for the collapse of a representative bubble are shown. The fluid surrounding the bubble is accelerated towards the bubble centre and the kinetic energy grows. Despite the very high bubble wall velocity at the end of the collapse the decrease of bubble volume is small and the fluid trying to fill the bubble is decelerated again. The begin t_{coll} of deceleration (transformation of kinetic energy in spray angle and surface) is regarded as begin of break-up of the primary ligament. The maximum kinetic energy is taken as amount of energy that a single bubble collapse contributes to the cavitation energy E_{cav} and t_{coll} is used as break-up time. Fig. 5(b) shows the maximum collapse energy during a single bubble collapse as function of initial bubble radius for the compressible case (conditions in Table 1) and for comparison also for the incompressible case (a = ∞, ρ = 360 kg/m^3). The curves of collapse energy per initial bubble volume are also given. For the compressible case the energy that is released by the collapse of a fixed vapour volume inside a primary ligament increases with increasing initial bubble radius between 1 µm and 20 µm and then keeps constant. Different bubble sizes result in different break-up energies and thus in different spray angles and secondary droplet sizes for the break-up of different primary ligaments. Comparing the energies of the compressible and the incompressible case the dominant influence of the sound speed is obvious. The use of incompressible bubble dynamics leads to an overestimation of break-up energy. Fig. 5(c) shows the bubble collapse time t_{coll} as function of initial bubble radius (compressible case). Collapse times are very short and result in a break-up very close to the nozzle (distance from nozzle in the range of nozzle hole diameter).

Turbulence modelling:

The turbulent kinetic energy k_0 and the dissipation rate ε_0 of each zone at the nozzle exit are known from the calculation of the nozzle flow. From the time the ligament leaves the nozzle until break-up the turbulent kinetic energy is reduced by dissipation. The simplified (no diffusion and production) 0-d k-ε model gives:

$$\frac{dk}{dt} = -\varepsilon \qquad (11a) \qquad \text{and} \qquad \frac{d\varepsilon}{dt} = -C_2 \frac{\varepsilon^2}{k} \qquad (11b) \quad . \tag{11}$$

Equations (11a) and (11b) can be solved analytical,

$$\left(\frac{\varepsilon}{\varepsilon_0}\right)=\left(\frac{k}{k_0}\right)^{C_2} \quad (12a)\,, \qquad \left(\frac{k}{k_0}\right)^{(1-C_2)} = \frac{(C_2-1)\varepsilon_0}{k_0}\,t+1 \quad (12b) \quad . \tag{12}$$

Using equation (12b) the actual value $k(t_{coll})$ available for break-up can be estimated.

Model validation

The new primary break-up model has been implemented in the KIVA-3Vcode. The calculation presented in this paper is done for geometry B. Diesel fuel (rail pressure: 65 MPa, 25°C) is injected in compressed air (5 MPa, 25°C, injection duration: 3 ms). The empirical constant κ = 0,003 (eq. (2)) gives good results for 5 MPa back pressure. The constants of the Kelvin-Helmholtz model are B_0 = 0,61 and B_1 = 25.

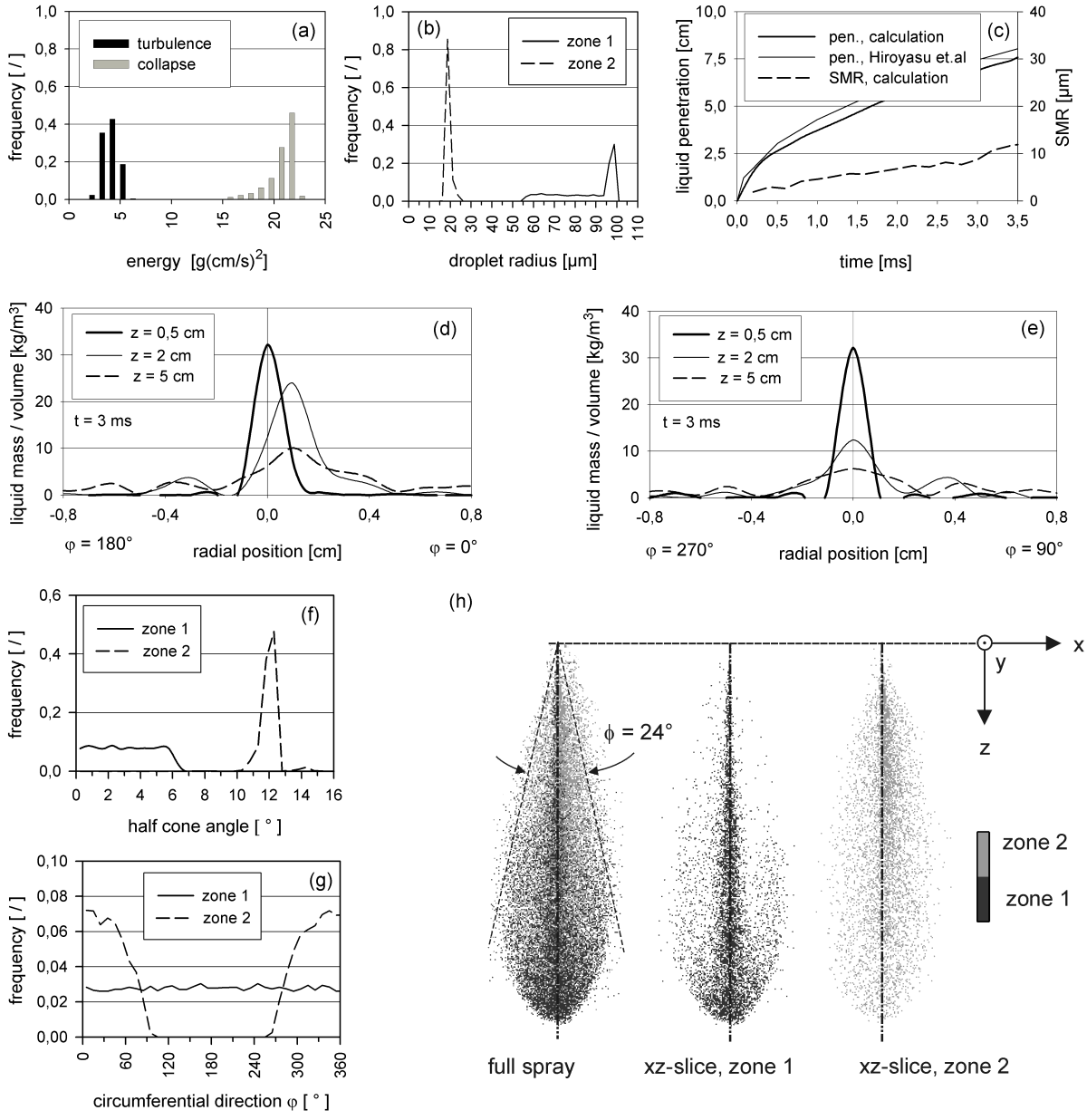

Figure 6: Geometry B: (a): Distribution of energy inside the primary ligaments before break-up,
(b): Distribution of secondary droplet radius, (c): Spray penetration and SMR ,
(d), (e): Radial distribution of liquid at different distances from the nozzle,
(f): Primary spray angle of secondary parcels, (g): 3-d-distribution of parcels,
(h): Distribution of droplets from zone 1 and zone 2 (full spray and 4 mm slices including the x-z-plane)

Fig. 6(a) shows the distribution of turbulent kinetic energy (from nozzle hole flow) and collapse energy for the 5000 primary parcels injected during the calculation. The bigger part of the total energy available for break-up of a ligament is collapse energy. Fig. 6(b) and 6(f) show the distributions of droplet sizes and primary spray angles for zone 1 and 2. Zone 2 with the highest break-up energy per unit mass disintegrates into smaller droplets than zone 1 and also has a larger primary spray angle. As imposed by the model, the concentration of the cavitation zone at the upper wall (265°>φ>95°) prevents secondary parcels of zone 2 to be created between φ = 95° and φ = 265° while secondary parcels of zone 1 are created at all circumferential positions (Fig. 6(g)). All in all this results in a 3-d asymmetric spray. Fig. 6(d) and 6(e) show the distribution of liquid on the two lines φ = 180°/0° and φ = 270°/90° through the spray at three distances z from the nozzle exit (for definition of φ see Fig. 4). As expected, the spray is symmetric on the line φ = 270°/90° and shows an asymmetric distribution on the line φ = 180°/0°. In Fig. 6(h) the picture of the full spray shows that a realistic spray angle is calculated. According to the experiments in [11] it should have a value of about 25°. The spray slices including the x-z-plane make clear that the droplets of zone 1 are symmetrically distributed while most of the droplets of zone 2 are on the right hand side (φ = 0°). Zone 2 governs the asymmetric distribution of liquid mass and spray angle near the nozzle. Zone 1 is responsible for the spray in the far field. Without zone 2 the resulting spray angle near the nozzle would be smaller. In Fig. 6(c) the curves of penetration and overall Sauter mean radius (SMR) are shown. The penetration is compared with the values of a semi-empirical equation for spray penetration developed by Hiroyasu and Arai [11]. The SMR has also reasonable values, the slight increase over time is a result of droplet collisions and coalescence.

The simulation of spray break-up for geometry A also gives reasonable results which are in the range of the ones described above and which are not shown in this paper. The main difference is that a symmetric spray is calculated.

Conclusion

A new model for cavitation and turbulence induced primary break-up has been developed, which is able to map the influence of the cavitating nozzle flow on spray break-up. Different locations and sizes of both vapour and liquid zones inside the injection holes lead to different spray structures and cone angles near the nozzle. The model includes cavitation bubble dynamics. The model describes the transition from the cavitating flow inside the injection hole to the dense spray near the nozzle and provides all necessary starting conditions for the spray simulation like spray cone angle, drop sizes, velocities etc. The model has been implemented in the 3-d-CFD code KIVA-3V and a first validation has been done. The model produces reasonable results for overall SMR, penetration, spray angle and mass distribution. Further validation with experimental data has to be done.

References

[1] Su, T.F., Chang, C.T., Reitz, R.D., Farrell, P.V., *Effects of Injection Pressure and Nozzle Geometry on Spray SMD and D.I. Emissions*, SAE 952360, 1995

[2] Bode, J., *Zum Kavitationseinfluß auf den Zerfall von Flüssigkeitsfreistrahlen*, Dissertation, Universität Göttingen, 1991

[3] Tamaki, N., Shimizu, M., Hiroyasu, H., *Enhanced Atomization of a Liquid Jet by Cavitation in a Nozzle Hole*, Eight International Conference on Liquid Atomization and Spray Systems, Pasadena, CA, USA, 2000

[4] Chaves, H., Knapp, M., Kubitzek, A., Obermeier, F., Schneider, T., *Experimental Study of Cavitation in the Nozzle of Diesel Injectors Using Transparent Nozzles*, SAE-paper 950290, 1995

[5] Arcoumanis, C., Gavaises, M., French, B., *Effect of Fuel Injection Process on the Structure of Diesel Sprays*, SAE-paper 970799, 1997

[6] Huh, K.Y., Gosman, A.D., *A Phenomenological Model of Diesel Spray Atomization*, International Conference on Multiphase Flows '91-Tsukuba, Japan, 1991, pp. 515-518

[7] Nishimura, A., Assanis, D.N., *A Model for Primary Diesel Fuel Atomization Based on Cavitation Bubble Collapse Energy*, *8th Int. Conf.* on Liquid Atomization an Spray Systems, Pasadena, pp.1249-1256, 2000

[8] Baumgarten, C., Shi, Y., Merker, G.P., *Numerical and Experimental Investigations of Cavitating Flow in High Pressure Diesel Nozzles*, ILASS-Europe 2001, Zürich, pp.593-599, 2001

[9] Prosperetti, A., Lezzi, A., *Bubble Dynamics in a Compressible Liquid, Part 1. First-Order Theory*, J. Fluid Mech., vol. 168, pp. 457-478, 1986

[10] Knapp, R.T., Daily, J.W., Hammitt, F.G., *Cavitation*, McGraw-Hill Book Company, 1970

[11] Hiroyasu, H., Arai, M., *Structures of Fuel Sprays in Diesel Engines*, SAE-paper 900475, 1990